Microscopics of Superconductivity in Perovskite Oxides: Challenges, Hurdles and Enigmas
MISPOCHE-2020, 2020.5.4

Spin-orbit-coupled ferroelectric superconductivity and multiorbital effects in $SrTiO_3$

Kyoto University, Japan
Shota Kanasugi & Youichi Yanase

[1] SK and Y. Yanase, Phys. Rev. B **98**, 024521 (2018).
[2] SK and Y. Yanase, Phys. Rev. B **100**, 094504 (2019).

Background

- SC and competing order
  - Unconventional SC near magnetic QCP (Even parity)
    e.g.) cuprates ⇒ d-wave SC
  - Coexistence of SC and ferromagnetism
    e.g.) UGe_2 ⇔ spin-triplet p-wave SC

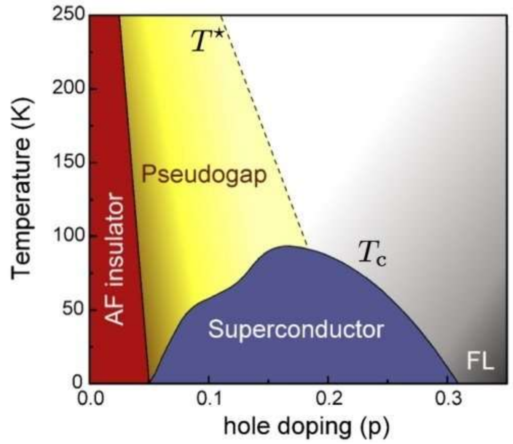

Phase diagram of high-T_c cuprates

- SC and ferroelectric order in $SrTiO_3$
  - SC at dilute density regime ⇔ unconventional pairing glue
  - Quantum paraelectric ⇔ vicinity of ferroelectric (FE) QCP (Odd parity)

Phase diagram for $Sr_{1-x}Ca_xTiO_{3-y}$

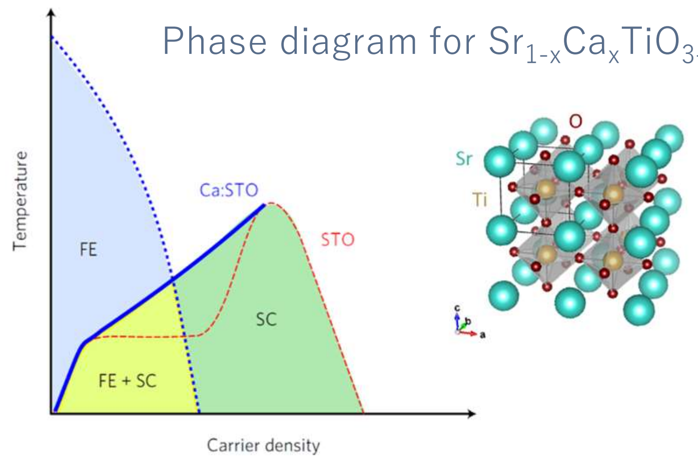

C. W. Rischau et al., Nat. Phys. **13**, 643 (2017).

SC and ferroelectricity:

competing or cooperating ?

Ferroelectricity and Rashba spin-orbit coupling

- Definition of metallic ferroelectricity

Lattice deformation
(real space)

SOC

Electronic state
(momentum space)

Paraelectric / Ferroelectric

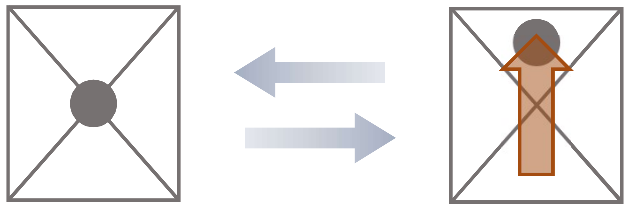

D_{4h} / C_{4v}

- Metal ⇒ Electric polarization is ill-defined.
- Ferroelectricity ≒ **Polar noncentrosymmetricity**

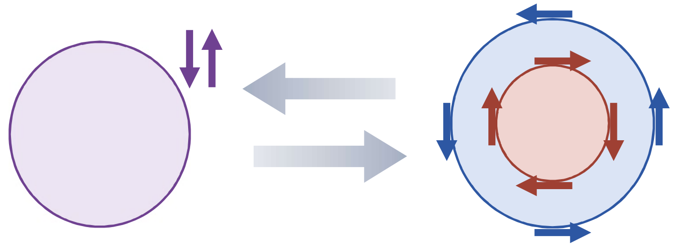

Polar crystal
⇓
Rashba SOC

$$\boldsymbol{g}(\boldsymbol{k}) = k_y\hat{\boldsymbol{x}} - k_x\hat{\boldsymbol{y}}$$

Metallic ferroelectricity ⇔ Spontaneous Rashba splitting of Fermi surfaces

Models

- Model1: 2D single-orbital Rashba model $\mathcal{H} = \mathcal{H}_{\rm kin} + \mathcal{H}_{\rm pol} + \mathcal{H}_{\rm pair} + \mathcal{H}_{\rm Z},$

$$\mathcal{H}_{\rm kin} = \sum_{\boldsymbol{k},s} [\varepsilon(\boldsymbol{k}) - \mu] c^\dagger_{\boldsymbol{k}s} c_{\boldsymbol{k}s},$$

Assumption: $\alpha \propto P$

$$\mathcal{H}_{\rm pol} = \sum_{\boldsymbol{k},s,s'} \alpha \boldsymbol{g}(\boldsymbol{k}) \cdot \hat{\boldsymbol{\sigma}}_{ss'} c^\dagger_{\boldsymbol{k}s} c_{\boldsymbol{k}s'},$$

// FE-induced Rashba SOC

G. Khalsa et al., PRB **86**, 125121 (2012).

$$= \frac{1}{N} \sum_{\boldsymbol{k},\boldsymbol{k}',\boldsymbol{q}} V(\boldsymbol{k},\boldsymbol{k}') c^\dagger_{\boldsymbol{k}\uparrow} c^\dagger_{-\boldsymbol{k}+\boldsymbol{q}\downarrow} c_{-\boldsymbol{k}'}$$

// s-wave pairing interaction

$$\mathcal{H}_{\rm Z} = -\mu_{\rm B} \sum_{\boldsymbol{k},s,s'} \boldsymbol{H} \cdot \hat{\boldsymbol{\sigma}}_{ss'} c^\dagger_{\boldsymbol{k}s} c_{\boldsymbol{k}s'},$$

// Zeeman magnetic field

Energy of polar lattice distortion

$$\mathcal{F}_{\rm lat}[P] = \frac{1}{2}\kappa_2 P^2 + \frac{1}{4}\kappa_4 P^4 + \frac{1}{6}\kappa_6 P^6$$

$$\mathcal{F}[\Delta, P] = \mathcal{F}_{\rm ele}[\Delta, P] + \mathcal{F}_{\rm lat}[P]$$

- Model2: 3D three-orbital t_{2g} model for $SrTiO_3$

$$\zeta_{yz,xz}(\boldsymbol{k}) = 2i\gamma \sin k_{x,y}$$

$$\mathcal{H}_0 = \sum_{\boldsymbol{k},l,\sigma} (\varepsilon_l(\boldsymbol{k}) - \mu) c^\dagger_{\boldsymbol{k},l\sigma} c_{\boldsymbol{k},l\sigma} + \lambda \sum_i \boldsymbol{L}_i \cdot \boldsymbol{S}_i + \sum_{\boldsymbol{k},\sigma} \sum_{l=yz,xz} [\zeta_l(\boldsymbol{k}) c^\dagger_{\boldsymbol{k},l\sigma} c_{\boldsymbol{k},xy\sigma} + {\rm H.c.}]$$

$\gamma \propto P$

- Rashba SOC = LS coupling × orbital parity mixing

YY and Sigrist, J. Phys. Soc. Jpn. 77, 124711 (2008).

Z. Zhong, A. Toth, and K. Held, Phys. Rev. B 87, 161102(R) (2013).

Minimal 2D model: High density regime

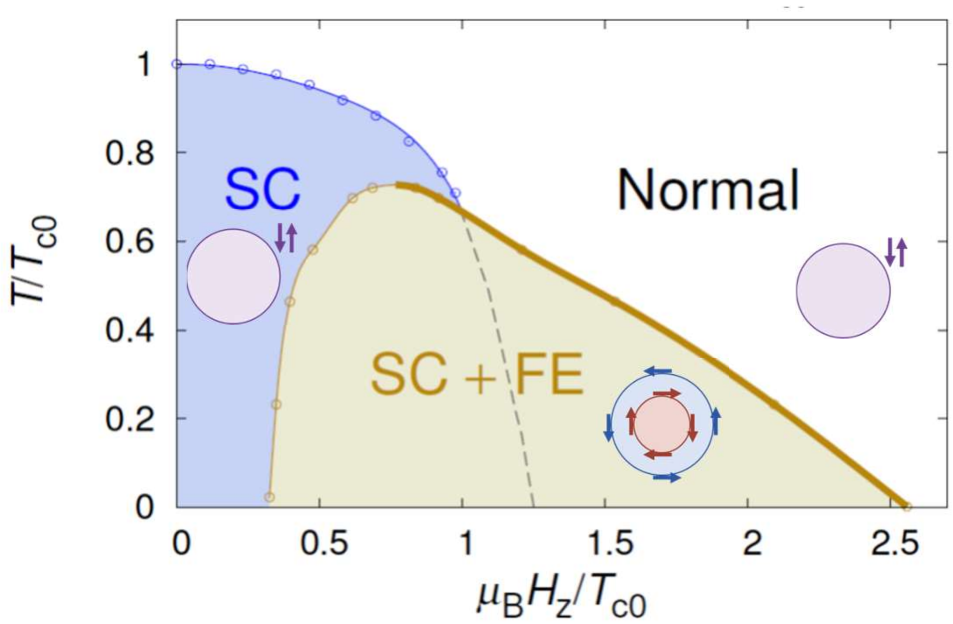

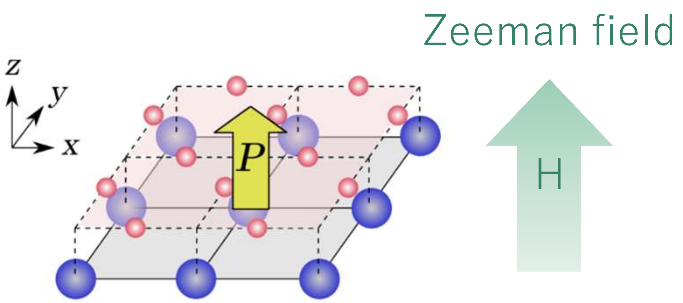

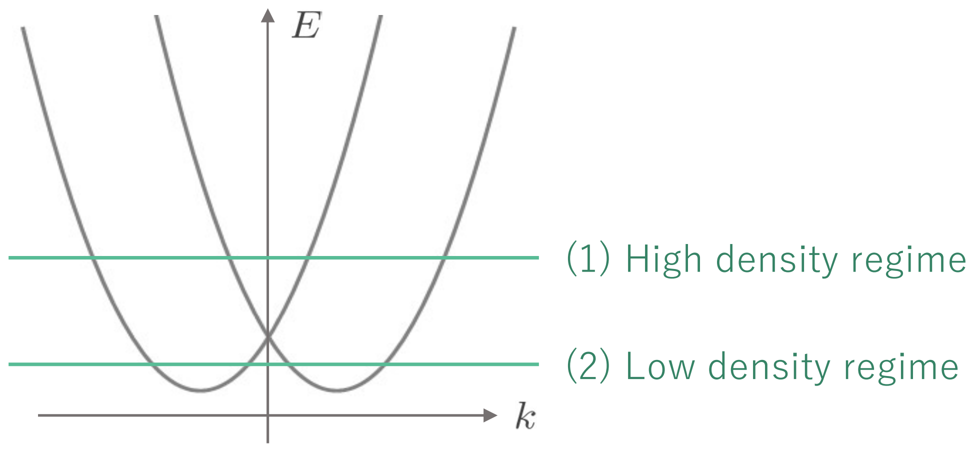

SC and FE: competing at H=0
cooperating at high H
due to anomalous Pauli depairing effect

Zeeman field → stabilization of FE order in SC state

"Superconducting multiferroics"

Minimal 2D model: Low density regime

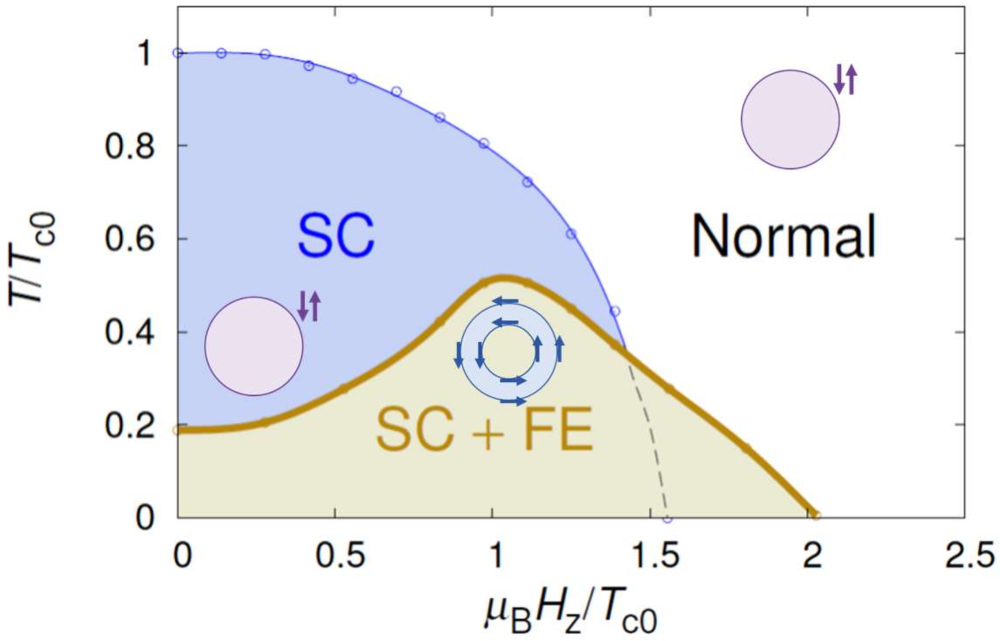

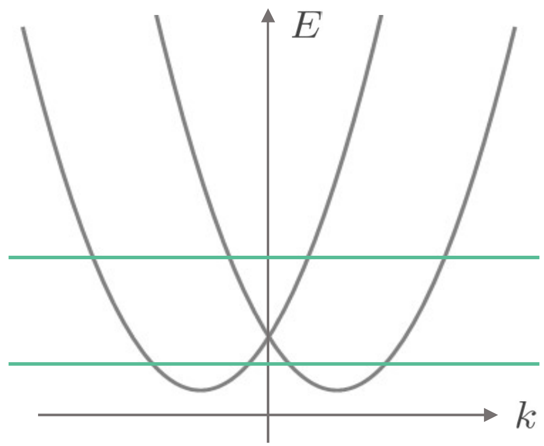

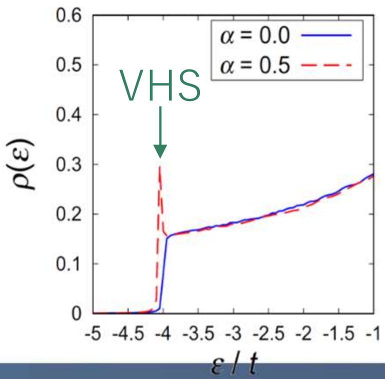

VHS due to
Lifshitz transition

SC and FE: cooperative at all H

Low density → FESC state w/o Zeeman field

S. Kanasugi and YY, Phys. Rev. B **98**, 024521 (2018).

3D t_{2g} model for $SrTiO_3$

▸ Multiorbital model for bulk STO

$$\zeta_{yz,xz}(\boldsymbol{k}) = 2i\gamma \sin k_{x,y}$$

$$\mathcal{H}_0 = \sum_{\boldsymbol{k},l,\sigma} (\varepsilon_l(\boldsymbol{k}) - \mu) c^\dagger_{\boldsymbol{k},l\sigma} c_{\boldsymbol{k},l\sigma} + \lambda \sum_i \boldsymbol{L}_i \cdot \boldsymbol{S}_i + \sum_{\boldsymbol{k},\sigma} \sum_{l=yz,xz} [\zeta_l(\boldsymbol{k}) c^\dagger_{\boldsymbol{k},l\sigma} c_{\boldsymbol{k},xy\sigma} + \mathrm{H.c.}]$$

- Three band structure originated from Ti: t_{2g} orbials
- Rashba SOC = LS coupling × orbital parity mixing
- Unconventional spin-orbital tex

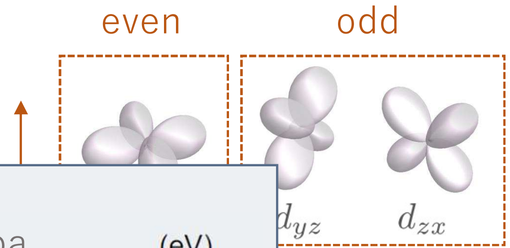

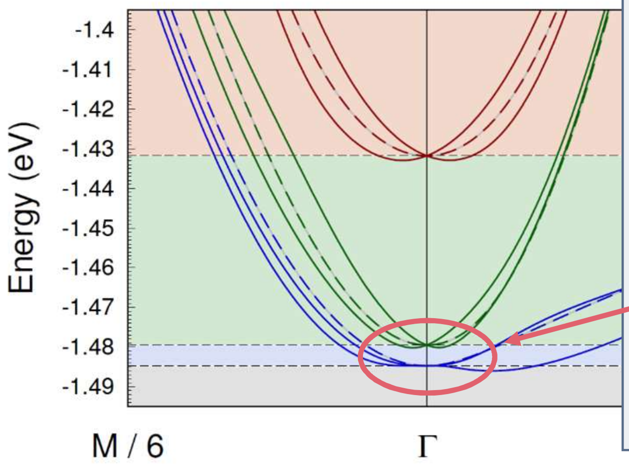

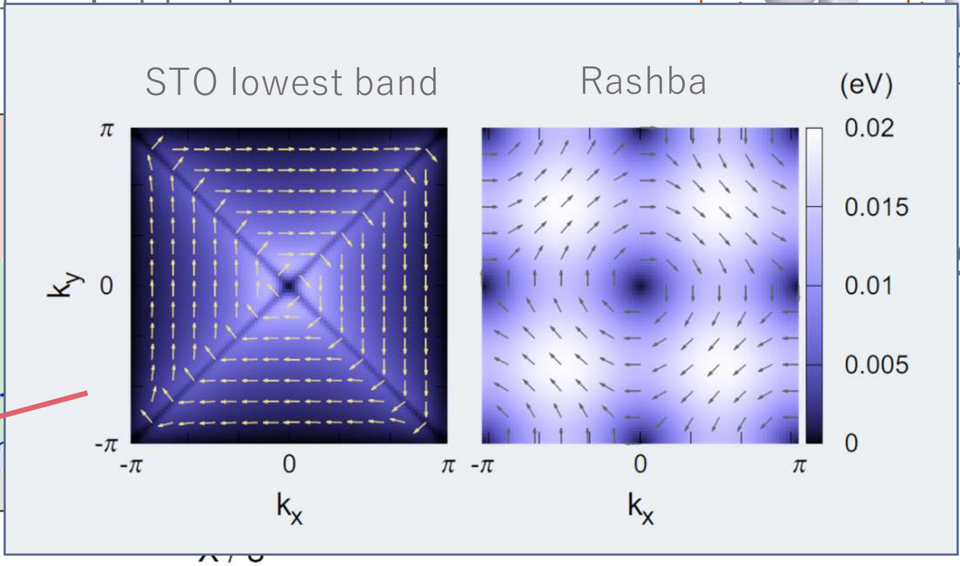

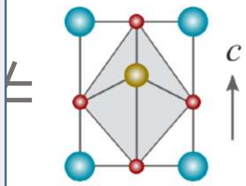

S. Kanasugi and YY, Phys. Rev. B **100**, 094504 (2019).

3D t_{2g} model for $SrTiO_3$

- Multiorbital effect on ferroelectric superconductivity

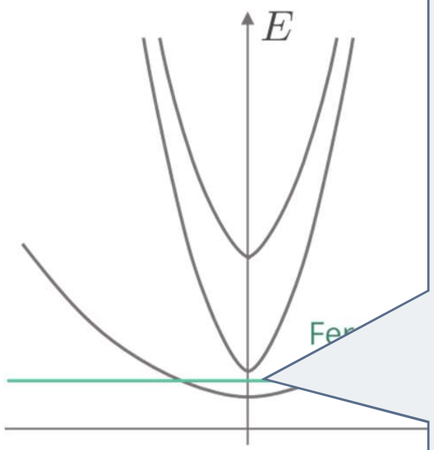

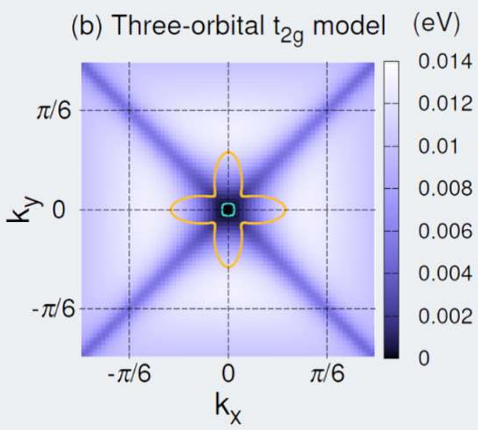

Strong Rashba SOC arises on the FS.

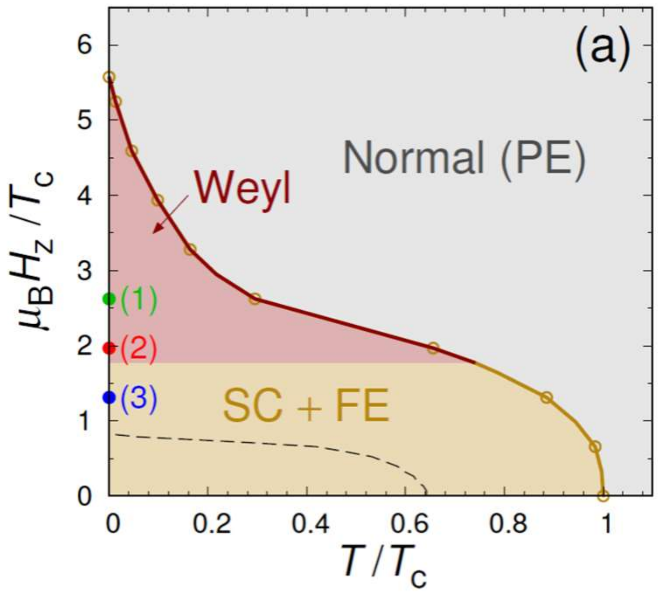

Assumption: intra-orbital static s-wave pairing interaction

- SC+FE phase is stabilized by the Lifshitz transition of the lowest band.
- Hc2 is drastically enhanced owing to the strong spin-momentum locking on FS.
- Topological Weyl SC state is stabilized in high-magnetic-field regime.

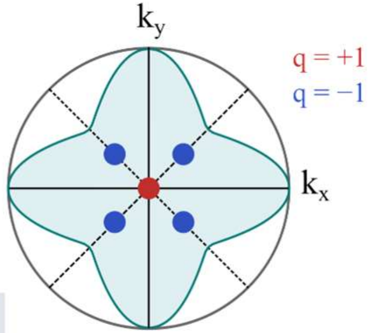

Dilute superconducting STO is a promising candidate of FESC and Weyl SC.

Classification of metallic multipole order

IR		Basis in real space	Basis in momentum space
A_{1g}	Q_{20}	z^2	k_z^2
	Q_{40}	z^4	k_z^4
	$Q_{44}^{\pm}$	$x^4-6x^2y^2+y^4$	$k_x^4-6k_x^2k_y^2+k_y^4$
		$xy(x^2-y^2)$	$k_xk_y(k_x^2-k_y^2)$
A_{2g}	Q_{44}^{-}	$xy(x^2-y^2)$	$k_xk_y(k_x^2-k_y^2)$
B_{1g}	Q_{22}^{+}	x^2-y^2	$k_x^2-k_y^2$
	Q_{42}^{+}	$(x^2-y^2)(7z^2-r^2)$	$(k_x^2-k_y^2)(7k_z^2-k^2)$
B_{2g}	Q_{22}^{-}	xy	k_xk_y
	Q_{42}^{-}	$xy(7z^2-r^2)$	$k_xk_y(7k_z^2-k^2)$
E_g	$Q_{21}^{\pm}$	$[zx, yz]$	$[k_zk_x, k_yk_z]$
	$Q_{41}^{\pm}$	$[zx(7z^2-3r^2), yz(7z^2-3r^2)]$	$[k_zk_x(7k_z^2-3k^2), k_yk_z(7k_z^2-3k^2)]$
	$Q_{43}^{\pm}$	$[zx(x^2-3y^2), yz(x^2-3y^2)]$	$[k_zk_x(k_x^2-3k_y^2), k_yk_z(k_x^2-3k_y^2)]$
A_{1u}	(Q_{54}^{-})	$xyz\,(x^2-y^2)$	$k_x\hat{\boldsymbol{x}}+k_y\hat{\boldsymbol{y}}+k_z\hat{\boldsymbol{z}}$ $k_z\hat{\boldsymbol{z}}-k_x\hat{\boldsymbol{x}}, k_z\hat{\boldsymbol{z}}-k_y\hat{\boldsymbol{y}}$
A_{2u}	Q_{10}	z	$k_y\hat{\boldsymbol{x}}-k_x\hat{\boldsymbol{y}}$
	Q_{30}	$z(5z^2-3r^2)$	
B_{1u}	Q_{32}^{-}	xyz	$k_x\hat{\boldsymbol{x}}-k_y\hat{\boldsymbol{y}}$
B_{2u}	Q_{32}^{+}	$z\,(x^2-y^2)$	$k_y\hat{\boldsymbol{x}}+k_x\hat{\boldsymbol{y}}$
E_u	$Q_{11}^{\pm}$	$[x, y]$	$[k_x\hat{\boldsymbol{z}}, k_y\hat{\boldsymbol{z}}], [k_z\hat{\boldsymbol{x}}, k_z\hat{\boldsymbol{y}}]$
	$Q_{31}^{\pm}$	$[x(5z^2-r^2), y(5z^2-r^2)]$	
	$Q_{33}^{\pm}$	$[x(x^2-3y^2), y(3x^2-y^2)]$	

T. Hitomi and YY, J. Phys. Soc. Jpn. 83, 114704 (2014).
L. Fu, Phys. Rev. Lett. 115, 026401 (2015).

Electric/magnetic multipole order parameter of tetragonal systems

Hexadecapole

Quadrupole

Dotriacontapole

Dipole

Octupole

Hikaru Watanabe and YY, Phys. Rev. B. **96**, 064432 (2017)

Superconductivity by k-space multipole fluctuations

TABLE IV. Solutions of the linearized gap equation (D6) for some multipole-fluctuation-mediated superconductivity in (a) D_{4h}, (b) D_{6h}, and (c) O_h crystalline systems. When there exist more than one solutions for a multipole fluctuation, they are listed in descending order of T_c. "MO" in (b) represents the magnetic octupole in momentum space [see Eq. (42)].

Γ	$\hat{\boldsymbol{k}}$-based multipole	IR	T_c	$\Delta(\boldsymbol{k})$	Fig.
			(a) Tetragonal (D_{4h})		
A_{2u}^{+}	$\hat{k}^x\hat{\boldsymbol{y}} - \hat{k}^y\hat{\boldsymbol{x}}$	A_{1g}	$1.14\omega_c \exp\left(-\frac{6\sqrt{30}-30}{N(0)\lvert V_0\rvert}\right)$	$[(\sqrt{30}-3)\{(\hat{k}^x)^2+(\hat{k}^y)^2\}+(12-2\sqrt{30})(\hat{k}^z)^2]i\sigma^y$	1(a)
		A_{2u}	$1.14\omega_c \exp\left(-\frac{3}{N(0)\lvert V_0\rvert}\right)$	$(\hat{k}^x\sigma^y - \hat{k}^y\sigma^x)i\sigma^y$	
E_u^{+}	$\{\hat{k}^y\hat{\boldsymbol{z}} \pm \hat{k}^z\hat{\boldsymbol{y}}, \hat{k}^x\hat{\boldsymbol{z}} \pm \hat{k}^z\hat{\boldsymbol{x}}\}$	A_{1g}	$1.14\omega_c \exp\left(-\frac{6(\sqrt{105}-10)}{N(0)\lvert V_0\rvert}\right)$	$[(12-\sqrt{105})\{(\hat{k}^x)^2+(\hat{k}^y)^2\}+(-18+2\sqrt{105})(\hat{k}^z)^2]i\sigma^y$	1(b)
		E_u	$1.14\omega_c \exp\left(-\frac{3\sqrt{2}}{N(0)\lvert V_0\rvert}\right)$	$\{(\sqrt{2}-1)(\hat{k}^x+i\hat{k}^y)\sigma^z \pm \hat{k}^z(\sigma^x+i\sigma^y),$ $(\sqrt{2}-1)(\hat{k}^x-i\hat{k}^y)\sigma^z \pm \hat{k}^z(\sigma^x-i\sigma^y)\}i\sigma^y$	
A_{2u}^{-}	$\hat{k}^z$	A_{1g}	$1.14\omega_c \exp\left(-\frac{9\sqrt{5}+15}{N(0)\lvert V_0\rvert}\right)$	$[(\sqrt{5}+3)\{(\hat{k}^x)^2+(\hat{k}^y)^2\}-2(\sqrt{5}+1)(\hat{k}^z)^2]i\sigma^y$	2(a)
E_u^{-}	$\{\hat{k}^x, \hat{k}^y\}$	A_{1g}	$1.14\omega_c \exp\left(-\frac{6\sqrt{30}+30}{N(0)\lvert V_0\rvert}\right)$	$[(\sqrt{30}+3)\{(\hat{k}^x)^2+(\hat{k}^y)^2\}-(12+2\sqrt{30})(\hat{k}^z)^2]i\sigma^y$	2(b)
			(b) Hexagonal (D_{6h})		
E_{1g}^{-}	$\{\hat{\boldsymbol{x}}, \hat{\boldsymbol{y}}\}$	no solution			
	MO	A_{1g}	$1.14\omega_c \exp\left(-\frac{534.451}{N(0)\lvert V_0\rvert}\right)$	$\{Y_{00}(\hat{\boldsymbol{k}}) - 0.478411Y_{20}(\hat{\boldsymbol{k}}) - 38.1751Y_{40}(\hat{\boldsymbol{k}})\}i\sigma^y$	3(a)
			(c) Cubic (O_h)		
E_g^{+}	$\frac{1}{2}\{2(\hat{k}^z)^2-(\hat{k}^x)^2-(\hat{k}^y)^2,$ $\sqrt{3}((\hat{k}^x)^2-(\hat{k}^y)^2)\}$	E_g	$1.14\omega_c \exp\left(-\frac{10}{N(0)\lvert V_0\rvert}\right)$	$\{2(\hat{k}^z)^2-(\hat{k}^x)^2-(\hat{k}^y)^2,$ $\sqrt{3}((\hat{k}^x)^2-(\hat{k}^y)^2)\}i\sigma^y$	
		A_{1g}	$1.14\omega_c \exp\left(-\frac{13.8864}{N(0)\lvert V_0\rvert}\right)$	$[Y_{00}(\hat{\boldsymbol{k}}) + 0.694319Y_{40}(\hat{\boldsymbol{k}})$ $+0.414935\{Y_{44}(\hat{\boldsymbol{k}})+Y_{4-4}(\hat{\boldsymbol{k}})\}]i\sigma^y$	3(b)
T_{1u}^{+}	$\{(\hat{\boldsymbol{k}}\times\boldsymbol{\sigma})^n\}$	A_{1g}	$1.14\omega_c \exp\left(-\frac{1}{N(0)\lvert V_0\rvert}\right)$	$i\sigma^y$	
		T_{1u}	$1.14\omega_c \exp\left(-\frac{6}{N(0)\lvert V_0\rvert}\right)$	$\{(\hat{\boldsymbol{k}}\times\boldsymbol{\sigma})^n i\sigma^y\}$	

S-wave SC is stable,
but P-wave SC has a similar T_c.

$$N(0)|V_0| \log\left(\frac{T_c^{A_{2u}}}{T_c^{A_{1g}}}\right) = (6\sqrt{30}-30) - 3 = -0.137,$$

In isotropic systems, T_c of p-wave SC is negligibly small.

$$N(0)|V_0| \log\left(\frac{T_c^{p\text{-wave}}}{T_c^{s\text{-wave}}}\right) = -5.$$

V. Kozii and L. Fu, Phys. Rev. Lett. **115**, 207002 (2015).
M. N. Gastiasoro, T. V. Trevisan, and R. M. Fernandes, arXiv:2001.04919

Shuntaro Sumita and YY, arXiv:2004.08086

Summary

- SC+FE phase in spin-orbit-coupled systems
  S. Kanasugi and YY, Phys. Rev. B **98**, 024521 (2018).
  - Metallic ferroelectricity can be characterized as spontaneous Rashba-splitting of FS.
  - High-density regime ⇒ SC+FE phase is stabilized under Zeeman field.
    ∵) Suppression of the Pauli depairing effect
  - Low-density regime ⇒ SC+FE phase is stabilized at zero field.
    ∵) Lifshitz transition of Fermi surface topology

- SC+FE phase & multiorbital effect in $SrTiO_3$
  S. Kanasugi and YY, Phys. Rev. B **100**, 094504 (2019).
  - Rashba SOC exhibits unconventional k-dependence due to multiorbital effect.
  - Strong Rashba spin-momentum locking in the dilute density regime.

Dilute STO is a promising candidate of FESC and Weyl SC.

Unresolved issues: Microscopic mechanism of superconductivity
Feedback effect on ferroelectric fluctuation
Orbital depairing at high density